Effects of Sb Adatoms on Kinetics of Electrocatalytic Oxidation of HCOOH at Sb-Modified Pt(100), Pt(111), Pt(110), Pt(320), and Pt(331) Surfaces—An Energetic Modeling and Quantitative Analysis

Yi-Yun Yang and Shi-Gang Sun*

State Key Laboratory for Physical Chemistry of Solid Surfaces, Department of Chemistry, Institute of Physical Chemistry, Xiamen University, Xiamen 361005, China

Received: June 7, 2002; In Final Form: September 26, 2002

Electrocatalytic oxidation of formic acid on Pt(100), Pt(110), Pt(111), Pt(320), and Pt(331) surfaces modified with Sb adatoms (Pt(*hkl*)/Sb) was investigated using cyclic voltammetry, potential step technique, and in-situ FTIR spectroscopy. Emphasis has been placed on investigations of the effects of Sb adatoms at Pt single-crystal surfaces on the kinetics of HCOOH oxidation. Quantitative data of kinetics of HCOOH oxidation via reactive intermediates were obtained by applying a potential step technique in combination with a data processing method of integration transform of $j-t$ transients, which has been described in our previous paper (Sun, S. G.; Yang, Y. Y. *J. Electroanal. Chem.* **1999**, *467*, 121). The current results illustrated that the kinetics of HCOOH oxidation is faster on bare surfaces of Pt(100), Pt(110), and Pt(320) than that on Sb-modified surfaces of these Pt single-crystal electrodes, but it is slower on bare surfaces of Pt(111) and Pt(331) than that on Sb-modified surfaces of the two Pt single-crystal electrodes. The peak potentials of HCOOH oxidation on Pt(*hkl*)/Sb were all converged in a narrow potential region between 0.20 and 0.30 V (SCE), implying that the adsorption of Sb on Pt(*hkl*) planes has altered the apparent activation energy of HCOOH oxidation. On the basis of quantitative results, we have proposed, for the first time, a rectifying factor of apparent activation energy (γ/kJ mol^{-1}) that describes the alteration by Sb adatoms of the apparent activation energy of HCOOH oxidation on Pt(*hkl*)/Sb surfaces. The values of γ have been determined quantitatively for $\gamma_{Pt(100)} = 12.80 \pm 0.317$, $\gamma_{Pt(110)} = 18.74 \pm 0.393$, $\gamma_{Pt(320)} = 16.683 \pm 0.349$, $\gamma_{Pt(111)} = -7.886 \pm 0.288$, and $\gamma_{Pt(331)} = -11.69 \pm 0.245$. The transfer coefficient β of HCOOH oxidation on the five Sb-modified Pt(*hkl*) electrodes was determined to be within the range of 0.12 ± 0.03, which is less dependent on the orientation of a Pt single crystal when it is modified with Sb adatoms and signifies a stepwise transfer of two electrons involved in HCOOH direct oxidation.

Introduction

Electrocatalytic oxidation of formic acid on different electrodes, such as Pt (polycrystalline and single crystal),[1−4] Au,[5,6] alloy,[7,8] modified surfaces,[9,10] etc., has been widely studied through cyclic voltammetry,[11,12] in-situ Fourier transform infrared spectroscopy (FTIRS),[13,14] differential electrochemical mass spectroscopy (DEMS),[15,16] and other methods,[17,18] owing to its importance in both fundamental electrocatalysis and applications in direct fuel cell. The kinetics of HCOOH oxidation was nevertheless not as extensively investigated because of difficulties arising from the so-called self-poisoning phenomenon,[4] which depicts the poisoning of an electrocatalyst by species derived spontaneously from the interaction of HCOOH or other small organic molecules with an electrode surface.[1,19] Sun et al.[4] have demonstrated first at the molecule level, by means of in-situ infrared spectroscopic studies, that the poisoning species generated from HCOOH interaction with Pt surfaces are CO adsorbates, and when these poisoning species have been removed by oxidation at higher potentials, HCOOH can be oxidized quickly into CO_2, i.e., the final oxidation product. This dual reaction mechanism of HCOOH oxidation was suggested initially by Parsons et al.,[1] and has been confirmed by several groups, recently by Weaver and coworkers.[20]

Our recent studies on the kinetics of dissociative adsorption[21] and direct oxidation[22] of HCOOH on Pt single-crystal electrodes (Pt(*hkl*)) demonstrated that the average rate of dissociative adsorption ($\bar{v}$) lies in the order of 10^{-10} mol cm^{-2} s^{-1}, and that the variation of $\bar{v}$ on Pt(*hkl*) versus electrode potential yields a volcano type curve on all Pt single-crystal electrodes investigated so far. On the basis of these results, the self-poisoning has been overcome successfully by designing a programmed potential step procedure, and kinetics parameters for HCOOH direct oxidation, i.e., the rate constant (k_f), the apparent activation energy ($\Delta H^{\ddagger\circ}$), and the transfer coefficient (β), have been determined by developing a data processing method of integration transform of $j-t$ transients.[22] Our results illustrated with quantitative data that the kinetics of both dissociative adsorption and direct oxidation of HCOOH depends strongly on the surface structure of Pt single-crystal electrodes. To learn more about the electrocatalytic properties of adatom-modified Pt single-crystal surfaces, we have recently studied oxidation of HCOOH on Sb adatom-modified Pt single-crystal electrodes (Pt(*hkl*)/Sb).[23,24] The results demonstrated that Sb adatoms on Pt(*hkl*) surfaces were able to suppress the formation of the poisoning species (i.e., CO adsorbates) to a great extent and to alter the

* Corresponding author. Tel: +86 592 2180181. Fax: +86 592 2183047. E-mail: sgsun@xmu.edu.cn.

10.1021/jp026260f CCC: $22.00
Published on Web 11/08/2002

catalytic activity of electrodes. Feliu and co-workers[25−27] also have reported some interesting and relevant results.

The present study is motivated by the idea that the adatoms could also have an important effect on surface reaction kinetics by affecting the apparent activation energy of direct oxidation of formic acid. The aim of this work is to provide insight into the effects of antimony adatoms on the direct oxidation of HCOOH at different orientations of a Pt single crystal by determining quantitatively kinetics parameters.

Experimental Section

To understand well the structural effects in electrocatalysis of HCOOH oxidation, five platinum single-crystal plans, Pt(100), Pt(110), Pt(111), Pt(320), and Pt(331), were prepared on the basis of a procedure described in our previous paper.[28] It is known[29] that the two high-index crystal plans, Pt(320) and Pt(331), belong, respectively, to [001] and [110] crystallographic zones, and their surface structure can be expressed as

$$\mathrm{Pt(320)} = \mathrm{Pt(s)}-[3(110)\times(100)]$$

$$\mathrm{Pt(331)} = \mathrm{Pt(s)}-[3(111)\times(111)]$$

i.e., the Pt(320) surface consists of terraces of 3 atomic rows of (110) symmetry and monatomic steps of (100) symmetry; the Pt(331) surface contains terraces of 3 atomic rows and monatomic steps both in (111) symmetry. The Pt single-crystal electrodes were treated using Clavilier's method[30] before each measurement, i.e., they were annealed in a hydrogen−oxygen flame, quenched with pure water, and transferred into an electrochemical cell under the protection of a droplet of pure water.

Irreversible adsorption (IRD) of Sb on Pt(100), Pt(110), Pt(111), Pt(320), and Pt(331) surfaces were carried out in 1 M H_2SO_4 solution containing 10^{-3} M Sb^{3+} ions. The electrodes after flame treatment were immersed in the solution for 1 min, rinsed with Millipore water, and transferred at 0.0 V to 0.5 M H_2SO_4 electrolyte in order to reduce Sb^{3+} into an Sb adatom (Sb_{ad}). Saturation coverage of Sb_{ad} was thus formed and determined. Starting from the saturation coverage of Sb_{ad}, different coverage of Sb_{ad} (θ_{Sb}) was obtained by partially stripping Sb_{ad} using cyclic voltammetry, in which the upper limit of potential scan (E_u) and the number of cycles of potential cycling were well-controlled. When the designated θ_{Sb} was calibrated in 0.5 M H_2SO_4, appropriate amounts of HCOOH were added, forming a 0.01 M HCOOH + 0.5 M H_2SO_4 solution for further study.

In-situ FTIR spectroscopic measurements were carried out with a Nexus 870 FTIR spectrometer (Nicolet) equipped with an EverGlo IR source and liquid nitrogen-cooled MCT-A detector. The spectral resolution was 16 cm^{-1}, and 400 interferograms in total were, respectively, collected at sample potential E_S and reference potential E_R. The resulting spectrum was calculated as $\Delta R/R = (R(E_S) - R(E_R))/R(E_R)$, where $R(E_S)$ and $R(E_R)$ are single-beam spectra acquired at E_S and E_R, respectively.

Solutions were prepared using Millipore water (18.0 MΩ cm) provided from a Milli-Q Lab apparatus (Nihon, Millipore Ltd.), super pure H_2SO_4, and analytical grade chemicals of HCOOH and Sb_2O_3. A saturated calomel electrode (SCE) served as the reference electrode. Potentials in this paper were all quoted versus this SCE reference. The solutions were deaerated with pure N_2 gas before the experiment for at least 20 min, and blanketed with an atmosphere of N_2 for the duration of the measurements to prevent possible interference of oxygen from the atmosphere. Experiments on the same Pt single-crystal plane were carried out under the same room temperature, around 20 °C.

Results and Discussion

1. Studies of Intrinsic Electrocatalytic Activity of Bare and Sb_{ad}-Modified Pt Single-Crystal Surfaces for HCOOH Oxidation. Oxidation of formic acid on platinum single-crystal electrodes can be employed as a model reaction in electrocatalysis.[4,31] Despite its simple molecule structure and only two electrons involved in its oxidation, the reaction occurred in a dual path mechanism on platinum electrodes as most small organic molecules did,[32] that is, the oxidation takes place either through reactive intermediates (R.I.) or via poisoning intermediates (P.I.). Both paths are sensitive to the surface structure of Pt electrocatalysts.[32,33]

The P.I. and the R.I. were determined mainly as CO and −COOH species in HCOOH oxidation, respectively, by using in-situ infrared spectroscopy.[4] As the oxidation via the R.I. route is a fast process, this path is often referred to as the direct oxidation of HCOOH.[31] The poisoning intermediates are derived from dissociative adsorption of HCOOH and can adsorb rather strongly on the Pt single-crystal surface at potentials below 0.45 V (vs SCE, in acid solutions), which poisons the electrode and inhibits the path of HCOOH oxidation via the reactive intermediates. Such a phenomenon has been known as the self-poisoning effect. To orient the oxidation via the R.I., i.e., the direct oxidation of formic acid, it is necessary to prevent the formation of the P.I. According to our previous investigations,[22−24] two ways may be used to fulfill such purpose: (1) using adatoms to modify electrodes surfaces; (2) designing a programmed potential step procedure, which can be used to study quantitatively the kinetics of HCOOH oxidation via the R.I. and will be described below.

We have demonstrated in previous papers[23,24] that the formation of P.I. can be inhibited by Sb adatoms on Pt single-crystal electrodes. Even at a low coverage of Sb_{ad} (θ_{sb}), the dissociative adsorption can be partially impeded. The electrocatalytic effect of Sb_{ad} toward HCOOH oxidation on Pt(100), Pt(110), Pt(111), Pt(320), and Pt(331) electrodes varied with θ_{sb}. The θ_{sb} that yields the maximum activity for HCOOH oxidation was determined, respectively, at 0.24 on Pt(100)/Sb, 0.13 on Pt(110)/Sb, 0.11 on Pt(111)/Sb, 0.023 on Pt(320)/Sb, and 0.020 on Pt(331)/Sb. The Sb adatoms formed through irreversible adsorption (IRA) are stable at potentials below 0.45 V on three base planes, below 0.40 V on Pt(320), and below 0.35 V on Pt(331).

To understand the effects of Sb adatoms on the kinetics of HCOOH oxidation, it is important to compare at first the intrinsic activity of bare and Sb_{ad}-modified Pt single-crystal electrodes. In recent years, we have developed a way to study the kinetics of both dissociative adsorption[21] and direct oxidation[22,23] of HCOOH on Pt single-crystal electrodes. For the sake of simplicity in illustration, we take the Pt(100) surface as an example to illustrate the methodology and results in this paragraph.

Figure 1 illustrates $j-E$ curves recorded in a positive-going potential scan (PGPS) for HCOOH oxidation at a bare Pt(100) and on Sb_{ad}-modified Pt(100) surfaces of different θ_{Sb}.[24] It can be seen that the oxidation current is almost near zero on the bare Pt(100) surface in the potential region between 0.0 and 0.50 V, which is ascribed to the self-poisoning phenomenon mentioned above and originates from dissociative adsorption of HCOOH on this surface.[4] However, significant oxidation

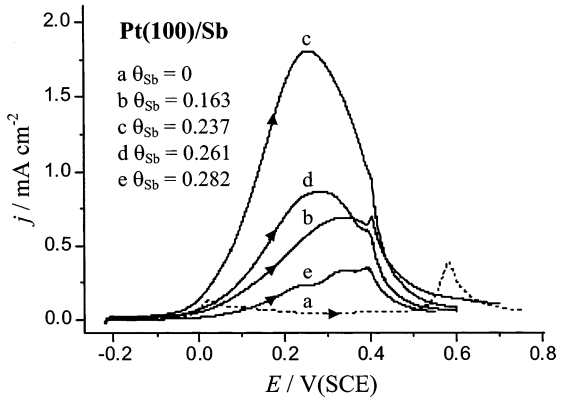

Figure 1. $j-E$ curves of HCOOH oxidation on bare Pt(100) (- − - − -) and Pt(100)/Sb of different θ_{Sb} (−) electrodes, 0.01 M HCOOH + 0.5 M H_2SO_4 solution, scan rate 50 mV s^{-1}.

TABLE 1: Comparison of the Peak Current Density (j_p) and the Peak Potential (E_p) of Formic Acid Oxidation on Bare Pt(*hkl*) and Pt(*hkl*)/Sb Electrodes, Data Measured from Figure 5 (see text for detail)

electrode		E_p/V (SCE)	j_p/mA cm^{-2}
Pt(100)	bare	0.20	5.206
	θ_{Sb}* = 0.237	0.25	1.808
Pt(320)	bare	0.10, 0.50	0.648, 2.534
	θ_{Sb}* = 0.0233	0.286	1.073
Pt(110)	bare	0.50	4.148
	θ_{Sb}* = 0.126	0.277	1.044
Pt(331)	bare	0.29, 0.50	0.432, 0.568
	θ_{Sb}* = 0.0203	0.256	1.252
Pt(111)	bare	0.15, 0.50	0.30, 0.29
	θ_{Sb}* = 0.114	0.293	0.565

current in the same potential region can be observed on Sb_{ad}-modified Pt(100) surfaces. Both potential (E_p) and amplitude of current density (j_p) of the current peak vary with θ_{Sb}. It is interesting to see that, at $\theta_{Sb} = 0.237$, the E_p stays at the lowest potential (0.25 V) and the j_p emerges with the highest value (1.81 mA cm^{-2}). This result indicates that the presence of a submonolayer of Sb adatoms on Pt(100) surface can enhance significantly the electrocatalytic activity for HCOOH oxidation in the PGPS, and the maximum enhancement was achieved at a critical θ_{Sb}, denoted as θ_{Sb}*. Similar results were obtained also on Pt(111), Pt(110), Pt(320), and Pt(331) surfaces;[24,34] the θ_{Sb}* and corresponding E_p and j_p obtained on the five Pt single-crystal electrodes are listed in Table 1 for comparison.

The in-situ FTIR spectroscopic results can reveal, at a molecule level, the effect of Sb adatoms on HCOOH oxidation. As shown in Figure 2, the in-situ FTIR spectrum recorded at a bare Pt(100) electrode in 0.01 M HCOOH + 0.1 M H_2SO_4 solution displays a bipolar band around 2040 cm^{-1}. This bipolar band can be assigned to the difference of IR absorption of linear bonded CO (CO_L) at E_R (−0.20 V) and E_S (−0.05 V). Since electrode potential remained at the potential of the open circuit (∼0.0 V) during IR alignment, the results indicate that HCOOH can be easily dissociated on the bare Pt(100) surface to form poisoning CO species, and that the adsorbed CO (CO_{ad}) is stable on the Pt(100) surface at −0.20 and −0.05 V. However, the CO_L band disappeared in spectra recorded under the same conditions on Sb_{ad}-modified Pt(100) surfaces as shown in Figure 2. Instead of the disappearance of the CO_L bipolar band, a strong negative-going band appears around 2345 cm^{-1}, which is ascribed to IR absorption of CO_2 species at −0.05 V. The in-situ FTIR results demonstrate that the oxidation of HCOOH has already been initiated on Sb_{ad}-modified Pt(100) surfaces at such low potentials, and that the oxidation of HCOOH is a fast

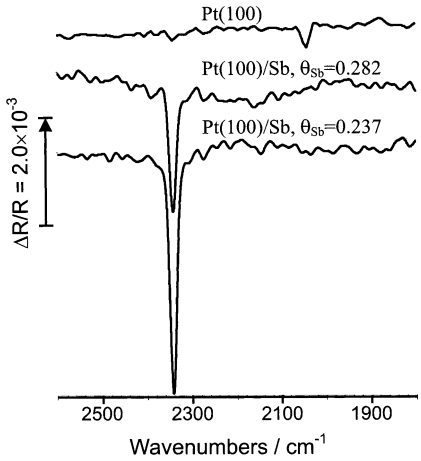

Figure 2. In-situ FTIR spectra recorded on bare Pt(100) and Pt(100)/Sb of different θ_{Sb} (0.237, 0.282) electrode in 0.01 M HCOOH + 0.1 M H_2SO_4 solution, $E_R = -0.20$ V, $E_S = -0.05$V.

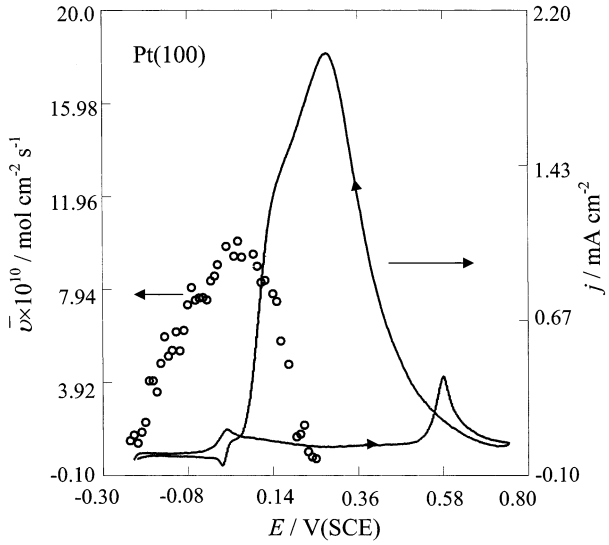

Figure 3. Comparison of cyclic voltammogram of HCOOH oxidation on a bare Pt(100) electrode (−) in 0.01 M HCOOH + 0.5 M H_2SO_4 solution with the distribution of the average rate (for a period of 1 min) of dissociative adsorption of HCOOH on a bare Pt(100) surface.

process which yields directly CO_2 (the final product) species. It is interesting to observe that the intensity of the CO_2 band in the spectrum of Pt(100)/Sb with $\theta_{Sb} = 0.237$, i.e., the θ_{Sb}*, is much larger than that in the spectrum of Pt(100)/Sb with $\theta_{Sb} = 0.282$. This result is in accordance with previous CV observations that the Pt(100)/Sb ($\theta_{Sb} = 0.237$) stays at the highest electrocatalytic activity for HCOOH oxidation.

A stable cyclic voltammogram of HCOOH oxidation at a bare Pt(100) is displayed in Figure 3. A large current peak appears in the $j-E$ curve recorded in the negative-going potential scan (NGPS). This illustrates that, when the poisoning CO_{ad} species have been removed by oxidation at potentials above 0.50 V, (a corresponding small current peak is observed in the PGPS), the HCOOH can be oxidized even in the NGPS in which a negative rate of potential variation is present. It is evident that the intrinsic activity of a bare Pt(100) surface for HCOOH oxidation may be measured from the $j-E$ curve recorded in the PGPS without self-poisoning. Such measurement could not be done, nevertheless, under normal cyclic voltammetric conditions due to the self-poisoning phenomenon. A programmed pulse voltammetry developed by Clavilier[35] may be one approach. To measure the intrinsic activity of bare Pt single-crystal electrodes, we have

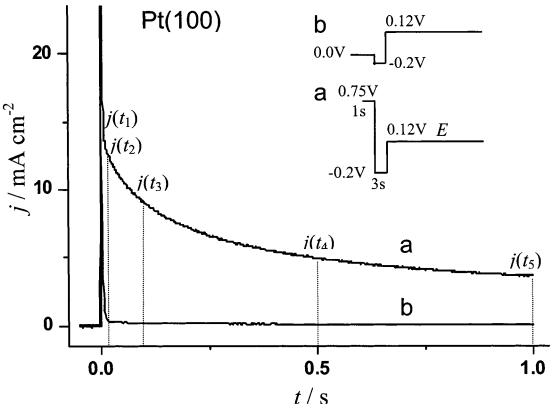

Figure 4. $j-t$ curves of HCOOH oxidation on a bare Pt(100) electrode, 0.01 M HCOOH + 0.5 M H_2SO_4 solution. Curves a and b were recorded with associate potential step program shown by inset a and b. The figure illustrated also the data sampling of $j(t)$ at $t = 0.01$, 0.05, 0.10, 0.50, and 1.0 s.

recently developed a programmed potential step technique[22] that was based on our studies of the kinetics of dissociative adsorption of HCOOH, i.e., the kinetics of HCOOH interaction with a bare Pt single-crystal electrode. The distribution with electrode potential of the average rate ($\bar{v}$) of HCOOH dissociative adsorption on a bare Pt(100) surface measured according to ref 22 is displayed in Figure 3. We can see that the variation of $\bar{v}$ with electrode potential manifests a volcano distribution. The maximum value of $\bar{v}$ locates around 0.05 V and the value of $\bar{v}$ tends toward zero when electrode potential is below −0.20 and above 0.20 V. On the basis of this knowledge, we have designed a program of potential step that can overcome effectively the self-poisoning and measure the intrinsic electrocatalytic activity of a bare Pt(100) surface for HCOOH oxidation.

As shown in Figure 4a(inset), the program of potential step consists of three parts: (1) the electrode potential was set first at 0.75 V and held for 1 s to remove all poisoning species except surface Pt oxide formed at this potential; (2) the electrode potential was stepped negatively to −0.20 V and held for 3 s to reduce surface Pt oxide and achieve the equilibrium state of solution in the vicinity of electrode surface; (3) the electrode potential was finally stepped to an oxidation potential, i.e., 0.12 V, and the current j of HCOOH oxidation was recorded immediately versus time t. As has been demonstrated in Figure 3 that the $\bar{v}$ tends toward zero at −0.20 V, the $j-t$ curve in Figure 4a should represent the intrinsic rate of HCOOH oxidation on the bare Pt(100) surface. For the sake of comparison, the $j-t$ curve in Figure 4b was recorded by applying the program b of the potential step (insert b to this figure). As a poisoning intermediate is formed on the Pt(100) surface at 0.0 V (i.e., close to the potential that yields the highest $\bar{v}$), the $j-t$ curve manifests practically no oxidation current except the current of double layer charging. The comparison of $j-t$ curves in Figure 4a and b illustrated clearly that the program a of potential step can overcome successfully the self-poisoning phenomenon, and can orient consequently the oxidation through the reactive intermediates, i.e., the direct oxidation of HCOOH on a bare Pt(100) surface. It is interesting to sample the $j-t$ curve of Figure 4a, i.e., taking the values of j at different t. The sampling data were denoted as $j(t_i)$. A series of programmed potential step experiments were carried out by varying the oxidation potential E. Therefore, the plot of $j(t_i)$ versus oxidation

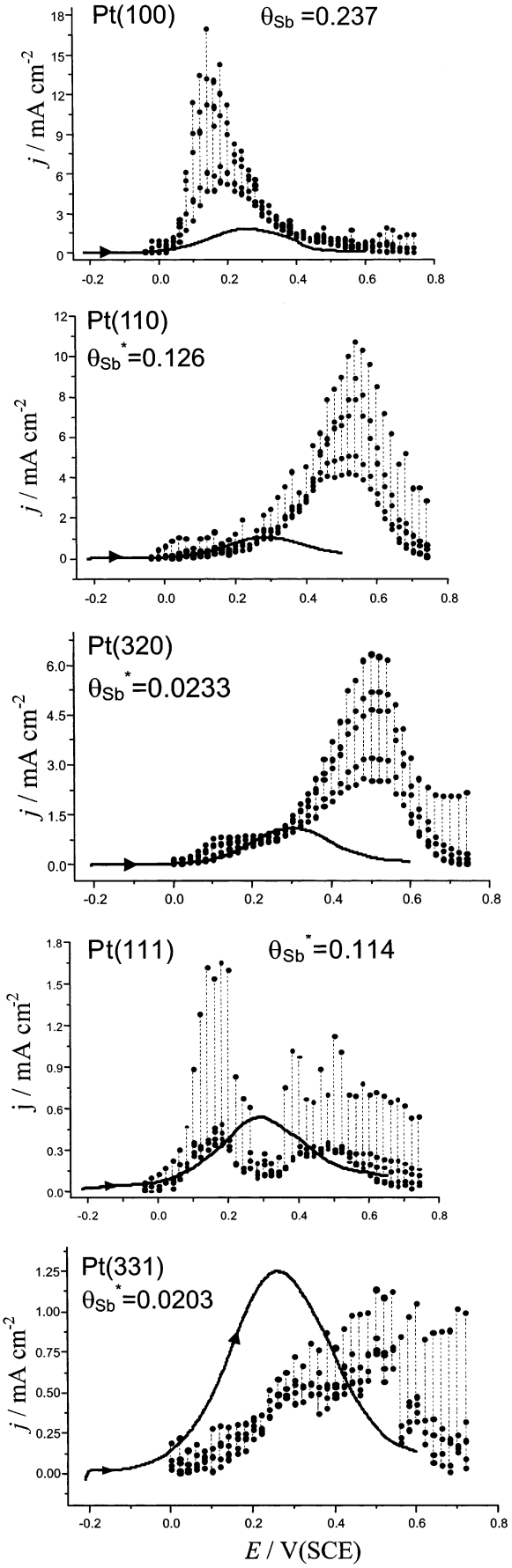

Figure 5. Comparison of the variations of $j(t)$ versus E acquired on bare Pt(hkl) with the $j-E$ curves recorded on Pt(hkl)/Sb of $\theta_{Sb} = \theta_{Sb}$*, 0.01 M HCOOH + 0.5 M H_2SO_4 solution.

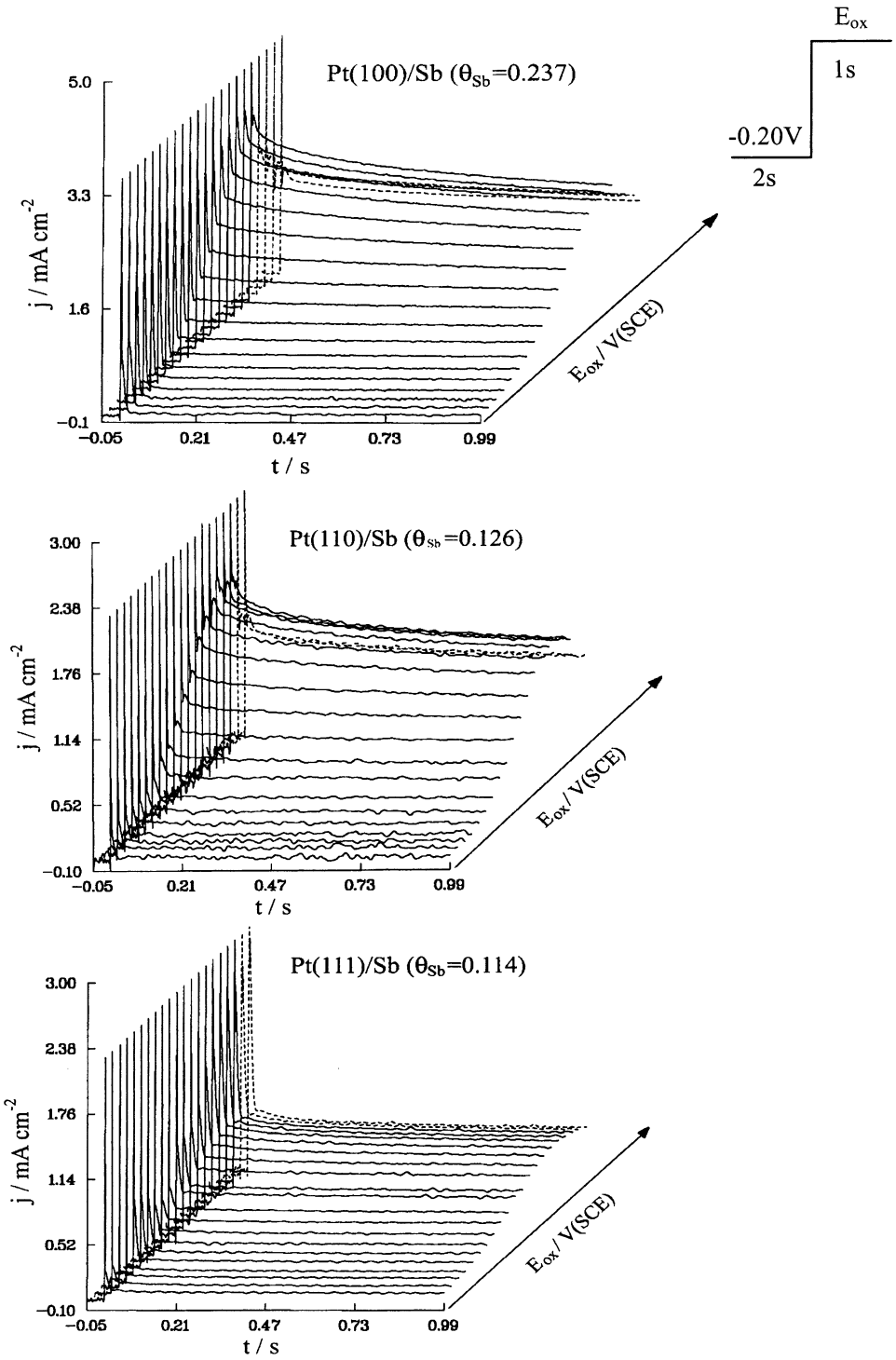

Figure 6. 3-D plots of $j-t-E$ for HCOOH oxidation on Pt(100)/Sb (θ_{Sb}* = 0.237), Pt(110)/Sb (θ_{Sb}* = 0.126), and Pt(111)/Sb (θ_{Sb}* = 0.114) electrodes, 0.01 M HCOOH + 0.5 M H_2SO_4 solution. The electrode potential was stepped from −0.20 V to different oxidation potentials E that varied from −0.04 to 0.40 V.

potential E represents, in fact, the variation of intrinsic electrocatalytic activity of a bare Pt(100) surface for HCOOH oxidation.

Figure 5 shows the comparison of $j(t_i)-E$ curves with $j-E$ curves recorded in the PGPS for HCOOH oxidation on the five Pt(*hkl*)/Sb($\theta_{Sb} = \theta_{Sb}$*) surfaces. Since the $j-E$ curve was obtained in a continuous potential scan, i.e, the electrode potential varied continuously, j may be considered as the quasi-stable activity of Pt(*hkl*)/Sb surface. It may be appropriate to take the value of $j(t = 1.0$ s) in the comparison, because $j(t =$ 1.0 s) has reached almost the stable current seen in the curve in Figure 4a. The quantitative results measured from Figure 5 are listed in Table 1. It is interesting to notice three significant changes when the Pt single-crystal surfaces were modified with Sb adatoms: (1) only one oxidation current peak appeared in the $j-E$ curves of the five Pt(*hkl*)/Sb($\theta_{Sb} = \theta_{Sb}$*) surfaces, while two oxidation current peaks can be seen in the $j(t_i)-E$ variations of bare Pt(320), Pt(331), and Pt(111); (2) the E_p varied from 0.10 to 0.50 V on the five bare Pt single-crystal surface, whereas the E_p has been converged to a narrow potential range, i.e., from 0.250 to 0.293 V, on the five Pt(*hkl*)/Sb($\theta_{Sb} = \theta_{Sb}$*) surfaces. This convergence may imply an alteration of apparent activation

energy of HCOOH oxidation by Sb adatoms; (3) the amplitudes of current peaks ($j_p^{Sb,max}$) for HCOOH oxidation on Pt(100)/Sb, Pt(320)/Sb, and Pt(110)/Sb are smaller than those on the corresponding bare surfaces, while the inverse situation occurred on Pt(111) and Pt(331) surfaces. As we have stated previously that the $j(t_i)-E$ variations in Figure 5 reflect the intrinsic properties of bare Pt(*hkl*) surfaces for HCOOH oxidation, the results of Figure 5 and Table 1 illustrated clearly two effects of Sb adatoms on Pt(*hkl*): (1) to alter the apparent activation energy of HCOOH oxidation; (2) to enhance the electrocatalytic activity of (111) surface sites (i.e., Pt(111) and Pt(331)), and to decrease the electrocatalytic activity of (100) and (110) surface sites (i.e., Pt(100), Pt(320), and Pt(110)).

2. Modeling of the Effects of Sb Adatoms on Pt Single-Crystal Surfaces and Methodology of Data Processing. As we have demonstrated by in-situ FTIRS data that the oxidation of HCOOH on Pt(*hkl*)/Sb surfaces can be considered as the direction oxidation, i.e., via the reactive intermediates, which involves a two-electron-transfer process, i.e.,

$$HCOOH + Pt/Sb_{ad} \rightarrow CO_2 + 2H^+ + 2e^- \qquad (1)$$

The transient oxidation current responding to a potential step from −0.20 V to an oxidation potential (as shown by the insert to Figure 6) may be written as[36]

$$j = 2FC_{HCOOH}k_f \exp\left(\frac{k_f^2 t}{D}\right)\mathrm{erfc}\left[k_f\left(\frac{t}{D}\right)^{1/2}\right] \qquad (2)$$

where D is the diffusion coefficient, F is the Faraday constant, and k_f is the rate constant that is expressed as

$$k_f = A \exp\left(-\frac{\Delta H^{\ddagger\circ}}{RT}\right)\exp\left(\frac{\beta nFE}{RT}\right) \qquad (3)$$

with $\Delta H^{\ddagger\circ}$ the apparent activation energy of HCOOH oxidation, β the transfer coefficient, and A the frequency factor.

As both E_p and j_p of HCOOH oxidation on Pt(100)/Sb (also on other Pt(*hkl*)/Sb surfaces) varied with θ_{Sb}, and the results of Figure 5 and Table 1 suggested an alteration of the apparent activation energy of HCOOH oxidation by Sb adatoms, we propose therefore a rectifying factor of activation energy (γ/kJ mol^{-1}) that describes the variation (Figure 1) of the apparent activation energy by the modification of Sb adatoms on Pt(*hkl*) surfaces. The k_f is thus modified by introducing γ,

$$k_f = A \exp\left(-\frac{\Delta H^{\ddagger\circ} + \gamma\theta_{Sb}}{RT}\right)\exp\left(\frac{\beta nFE}{RT}\right) \qquad (4)$$

Equation 4 can be also written as

$$k_f = k^{\circ\prime} \exp\left(\frac{\beta nFE}{RT}\right) \qquad (5)$$

with

$$k^{\circ\prime} = A \exp\left(-\frac{\Delta H^{\ddagger\circ} + \gamma\theta_{Sb}}{RT}\right) \qquad (6)$$

According to the above analysis, the data processing procedure may be performed in following steps:

(1) Starting from $j-t$ transient curves of HCOOH oxidation on Pt(*hkl*)/Sb electrodes with different θ_{Sb}, the rate coefficient $k_f(E, \theta_{Sb})$ can be determined by using the method of integration transform of $j-t$ transient data;[22]

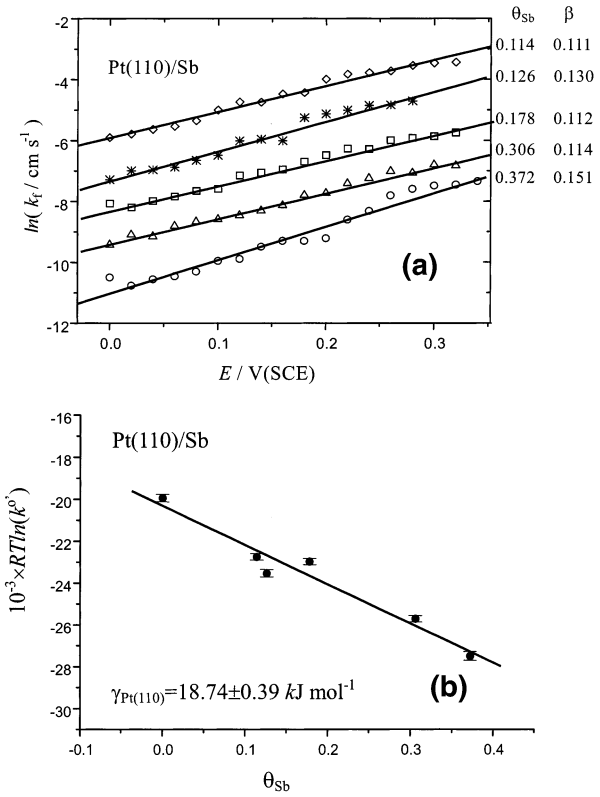

Figure 7. (a) Variation of ln(k_f) against E at different θ_{Sb}; (b) Plot of ln($k^{\circ\prime}$) versus θ_{Sb}, Pt(110)/Sb electrode, 0.01 M HCOOH + 0.5 M H_2SO_4 solution.

(2) Obtaining $k^{\circ\prime}$ and β at each θ_{sb} through regression of ln(k_f) versus E, i.e.,

$$\ln(k_f) = \ln(k^{\circ\prime}) + \beta nFE/RT \qquad (7)$$

(3) Acquiring finally the rectifying factor γ from the regression of ln($k^{\circ\prime}$) against θ_{Sb},

$$RT\ln(k^{\circ\prime}) = (RT\ln(A) - \Delta H^{\ddagger\circ}) - \gamma\theta_{Sb} \qquad (8)$$

3. Investigation of Kinetics of HCOOH Oxidation on Sb_{ad}-Modified Pt Single-Crystal Electrodes. Figure 6 illustrates the variation of $j-t$ transients with E for HCOOH direct oxidation on Pt(100)/Sb(θ_{Sb}*), Pt(110)/Sb(θ_{Sb}*), and Pt(111)/Sb(θ_{Sb}*) electrodes. The electrode potential was stepped directly from −0.2 V to a different oxidation potential E that was varied from −0.04 to 0.40 V. Since Sb adatoms on these Pt single-crystal surfaces have suppressed the dissociative adsorption of HCOOH, i.e., the self-poisoning phenomenon has been avoided, we can see immediately that the $j-t$ transients in Figure 6 are oxidation current of HCOOH on these electrodes. It is evident that three factors will affect the $j-t$ transient behaviors: the surface structure of the Pt(*hkl*)/Sb electrode, the oxidation potential, and the coverage of Sb adatoms.

By employing the data processing method of integration transform of $j-t$ transients,[22] the values of k_f can be calculated from the $j-t$ transients in Figure 6. The k_f evaluated from $j-t$ transients recorded on Pt(110)/Sb electrodes with different θ_{sb} and at different oxidation potentials are plotted in Figure 7a, in which the scale of the Y-axis corresponds to $\theta_{sb} = 0.372$, and for convenience of observation the plots of ln(k_f) versus E at other θ_{sb} values are shifted up gradually. From each plot at a given θ_{sb} we obtain β and ln($k^{\circ\prime}$) through linear regression according to eq 7, the values of β are listed also in the figure.

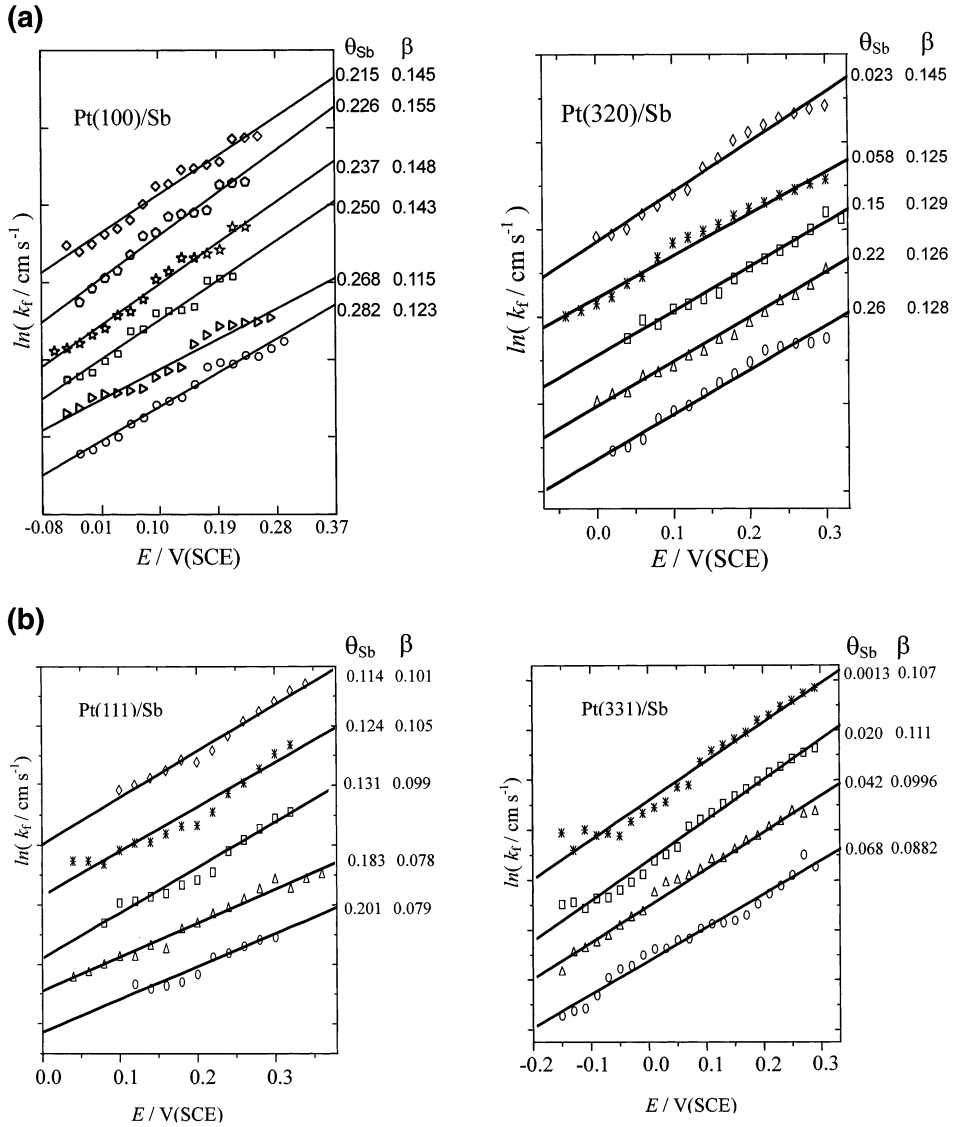

Figure 8. Variations of ln(k_f) against E at different θ_{Sb} on (a) Pt(100)/Sb, Pt(320)/Sb, and (b) Pt(111)/Sb, Pt(331)/Sb electrodes; 0.01 M HCOOH + 0.5 M H_2SO_4 solution.

The transfer coefficient β represents the influence extents of the activation free energy of the electrochemical reaction by electrode potential.[36,37] We noticed that the values of β listed in Figure 7a range between 0.11 and 0.15. The average value of β is 0.123, and it is much smaller than the normal value 0.50 for a reversible reaction of simple charge transfer. This result may indicate a stepwise transfer of two electrons, and may also imply that the oxidation of HCOOH is a complex reaction that involves interaction of HCOOH molecules with the electrode surface.[22] In comparing the value of β obtained on Pt(110)/Sb_{ad} with that obtained on a bare Pt(110) electrode ($\beta = 0.102$),[23,24] the value of β increased when Sb adatoms are present on the Pt(100) surface, which may be an illustration that the electronic structure of Pt(110) electrode has been altered by the modification of Sb adatoms. The above results demonstrated that after the modification of Pt(110) electrode with Sb adatoms, the surface composition and structure were both modified. As a consequence, the electrocatalytic activity of the electrode for HCOOH oxidation has been affected.

The variation of $RT \ln(k^{\circ\prime})$ versus θ_{Sb} is shown in Figure 7b. According to eq 8 the linear regression between $RT \ln(k^{\circ\prime})$ and θ_{Sb} will produce the rectifying factor of apparent activation energy for HCOOH oxidation on a Pt(110)/Sb electrode. The γ was thus evaluated from Figure 7b to be 18.74 kJ mol^{-1}. Using the methodology proposed by Oldham in ref 38, the relative error of calculation for the integration transformation of $j-t$ digital transient data under the present experimental conditions may be within 1% for a total 2500 data points.[22] Under this consideration the error in evaluation of γ should be the sum of the calculation error in the integration transform of $j-t$ digital transient data and the averaging standard error. So the total error in evaluating γ arises mainly from the error in integration transform of $j-t$ digital transient data ($\delta\gamma = 18.74 \times 1\% = 0.187$) plus the error in calculation of the $\ln(k^{\circ\prime})$ ($\delta\gamma = 0.206$), the sum of the two parts has been counted at 0.393 kJ mol^{-1}. We obtained finally $\gamma_{Pt(110)} = 18.74 \pm 0.393$ kJ mol^{-1}.

By applying the same experimental procedure and data processing method, the values of the rate constant k_f of HCOOH oxidation on Pt(100)/Sb, Pt(111)/Sb, Pt(320)/Sb, and Pt(331)/Sb electrodes at different potentials and different θ_{Sb} were evaluated. The results were represented by plots of ln(k_f) versus E and θ_{sb} in Figure 8. We observe that, on these four Pt(hkl)/Sb electrodes, the linearity between ln(k_f) and E at all θ_{Sb} values is maintained. Using the same procedure of data processing employed in analysis for HCOOH oxidation on Pt(110)/Sb electrode, $\ln(k^{\circ\prime})$ and β have been calculated at each θ_{sb} through linear regression according to eq 7 for HCOOH oxidation on

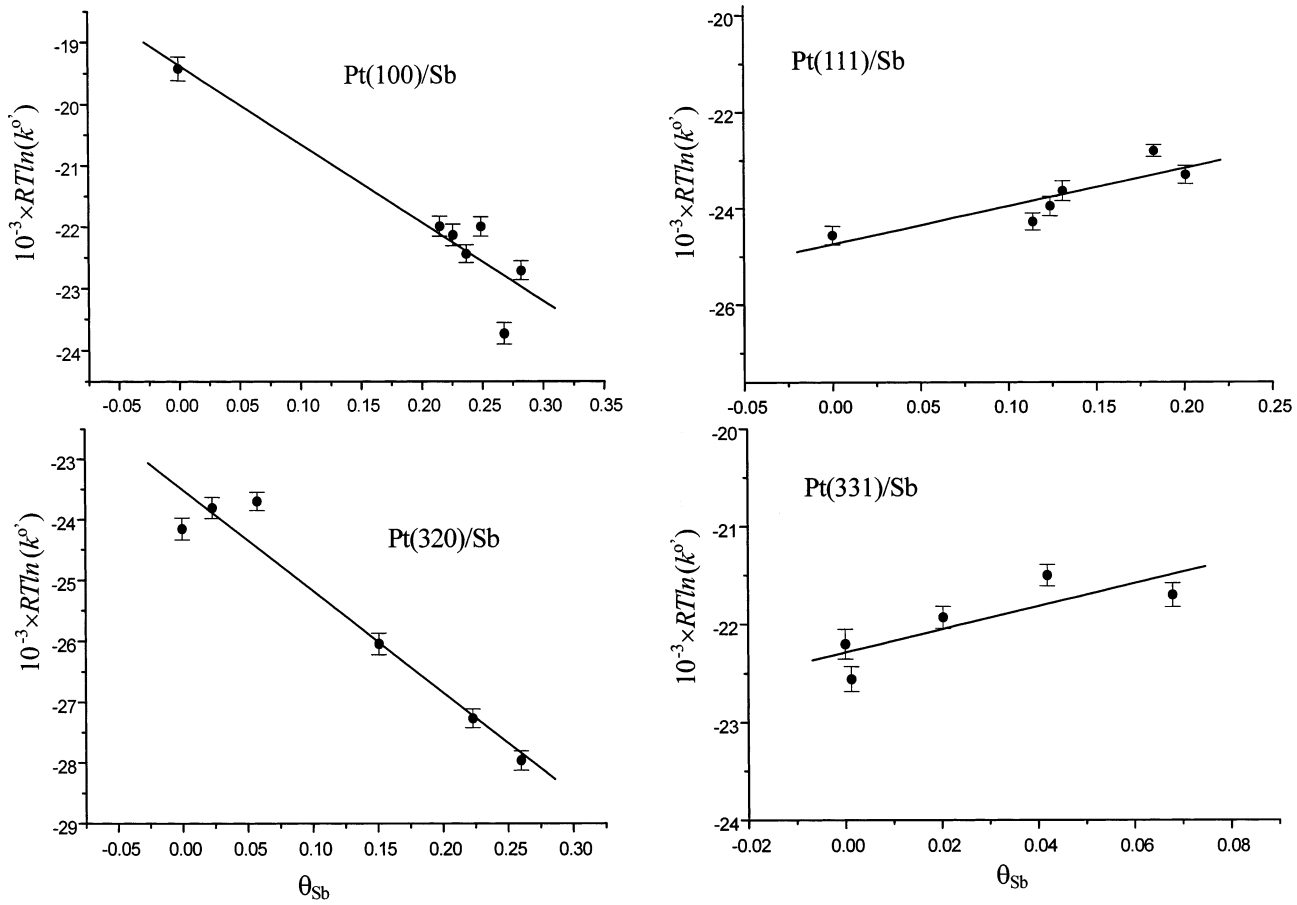

Figure 9. Plots of $\ln(k_f^{\circ\prime})$ versus θ_{Sb} on Pt(100)/Sb, Pt(320)/Sb, Pt(111)/Sb, Pt(331)/Sb electrodes, 0.01 M HCOOH + 0.5 M H_2SO_4 solution.

TABLE 2: Comparison of γ Determined on Different Pt(*hkl*)/Sb Electrodes

		consequences	
Pt(*hkl*)	γ/kJ mol^{-1}	$\Delta H^{\ddagger\circ} + \gamma\theta_{sb}$	j
Pt(100)	12.80 ± 0.32	↑	$j_p^{Sb,max} < j_p^{max}$
Pt(320) = (3(110)−(100))	16.68 ± 0.35	↑	$j_p^{Sb,max} < j_p^{max}$
Pt(110)	18.74 ± 0.39	↑	$j_p^{Sb,max} < j_p^{max}$
Pt(111)	-7.89 ± 0.29	↓	$j_p^{Sb,max} > j_p^{max}$
Pt(331) = (3(111)−(111))	-11.69 ± 0.24	↓	$j_p^{Sb,max} > j_p^{max}$

Pt(100)/Sb, Pt(111)/Sb, Pt(320)/Sb, and Pt(331)/Sb electrodes. The values of β are also given in Figure 8. We can see once again that the values of all β for HCOOH direct oxidation on these four Sb-modified Pt(*hkl*) electrodes are smaller than 0.15, confirming the irreversibility of HCOOH direct oxidation and a stepwise transfer of two electrons.

The plots of $\ln(k^{\circ\prime})$ versus θ_{sb} for HCOOH direct oxidation on Pt(100)/Sb, Pt(111)/Sb, Pt(320)/Sb, and Pt(331)/Sb electrodes are shown in Figure 9. We observe that each plot exhibits a linear relationship. Further regression analysis on $\ln(k^{\circ\prime})$ against θ_{sb} yielded the rectifying factor of apparent activation energy for HCOOH oxidation on each of the four Pt single-crystal electrodes modified with Sb adatoms. Table 2 summarizes the values and the corresponding evaluation errors of γ for HCOOH oxidation on Pt(100)/Sb, Pt(111)/Sb, Pt(320)/Sb, and Pt(331)/Sb electrodes. For convenience of comparison, the kinetics data obtained on a Pt(110)/Sb electrode are also listed in the same table.

From the data listed in Table 2, we may see that the γ obtained on Pt(100)/Sb, Pt(110)/Sb, and Pt(320)/Sb is positive, but it is negative on Pt(111)/Sb and Pt(331)/Sb. It is known that Pt(100), Pt(110), and Pt(320) contain mainly (100) and (110) surface sites and that Pt(111) and Pt(331) are composed mainly of (111) sites on their surfaces, the results of Table 2 illustrated that the γ is sensitive to surface structure of Pt single-crystal electrodes upon the modification of Sb adatoms. The positive value of γ demonstrated that the apparent activation energy ($\Delta H^{\ddagger\circ} + \gamma\theta_{Sb}$) of HCOOH oxidation would be increased by the presence of Sb adatoms. As a consequence, the intrinsic electrocatalytic activity of Sb-modified Pt(100), Pt(110), and Pt(320) surfaces will be lower than the corresponding bare electrodes. In contrast, the negative value signifies a decrease of ($\Delta H^{\ddagger\circ} + \gamma\theta_{Sb}$) by the modification of Sb. So the intrinsic electrocatalytic activity of Sb-modified Pt(111) and Pt(331) surfaces will be higher than the corresponding bare electrodes. The results of kinetics are in good agreement with the comparison of intrinsic electrocatalytic activity of Pt(*hkl*) and Pt(*hkl*)/Sb electrodes toward HCOOH oxidation described in Section 3.1.

Conclusions

The present study demonstrated, from the point of view of kinetics and for the first time, the effects of surface Sb adatoms on Pt single-crystal electrodes toward HCOOH oxidation via the reactive intermediates. The main achievements include three aspects: (1) It has revealed that the apparent activation energy of HCOOH oxidation has been altered by the presence of Sb adatoms on Pt single-crystal electrodes; (2) On the basis of experimental results, a rectifying factor of apparent activation energy (γ) has been proposed and determined quantitatively to describe the effect of Sb adatoms on the kinetics of HCOOH oxidation; (3) The rate constant (k_f), the transfer coefficient (β)

together with the γ were determined for HCOOH oxidation on Sb-modified Pt single-crystal electrodes of different Sb coverage.

The results illustrated that the values of k_f obtained from the linear regression of integral transformation of $j-t$ data at different potentials, at different θ_{Sb}, and on different Pt single-crystal electrodes all ranged from 10^{-4} to 10^{-3} cm s^{-1}. The linear relationship between $\ln(k_f)$ and E is maintained in a specified potential region on each Pt(*hkl*)/Sb electrode at all θ_{Sb} studied in the current paper. The fact that a good linearity between $\ln(k_f)$ and E is preserved demonstrated that the oxidation of HCOOH on Sb-modified Pt single-crystal electrodes occurred at surfaces free from self-poisoning. From the regression of $\ln(k_f)$ versus E, $\ln(k^{\circ\prime})$ and β have been evaluated out. The small values of β (almost in the range of 0.12 ± 0.03 on the five Pt(*hkl*)/Sb) may be representative for a stepwise transfer of two electrons involved in HCOOH oxidation. From the regression of $RT \ln(k^{\circ\prime})$ against θ_{Sb}, the rectifying factor of apparent activation energy (γ) of HCOOH oxidation on Pt(100)/Sb, Pt(110)/Sb, Pt(111)/Sb, Pt(320)/Sb, and Pt(331)/Sb has been finally calculated out. The values of γ on the five Pt(*hkl*)/Sb were determined quantitatively. The γ is positive on Pt(100)/Sb, Pt(110)/Sb, and Pt(320)/Sb, while it is negative on Pt(111)/Sb and Pt(331)/Sb. The negative values of γ result in a decrease of the apparent activation energy of HCOOH oxidation, indicating that the adsorption of Sb adatoms on Pt(111) and Pt(331) surfaces will enhance the electrocatalytic activity. While the positive values of γ give rise to an increase in the apparent activation energy of HCOOH oxidation when Pt(100), Pt(110), and Pt(320) surfaces are modified with Sb adatoms. As a consequence, the electrocatalytic activity will be dropped off. The experimental observations on the variation of current density of HCOOH oxidation on Pt(*hkl*)/Sb in comparison with that on corresponding bare Pt(*hkl*) are in good agreement with the prediction of γ values. The present results have thrown a new light upon revealing the origins of electrocatalytic effects of Sb adatoms, and upon understanding the surface structure effects of Sb-modified Pt single-crystal electrodes on the kinetics of HCOOH oxidation as well.

Acknowledgment. The present study was supported financially by grants of the National Natural Science Foundation of China (NSFC) and Education Ministry of China.

References and Notes

(1) Capon, A.; Parsons, R. *J. Electroanal. Chem.* **1973**, *44*, 239.
(2) Jiang, J. H.; Kucernak, A. *J. Electroanal. Chem.* **2002**, *520*, 64.
(3) Bernasek, S. L.; Somorjai, G. A. *Surf. Sci.* **1975**, *48*, 204.
(4) Sun, S. G.; Clavilier, J.; Bewick, A. *J. Electroanal. Chem.* **1988**, *240*, 147.
(5) Xiang, J.; Wu, B. L.; Chen, S. L. *J. Electroanal. Chem.* **2001**, *517*, 95.
(6) Avramov-Ivic, M.; Strbac, S.; Mitrovic, V. *Electrochim. Acta* **2001**, *46*, 3175.
(7) Markovic, N. M.; Gasteiger, H. A.; Ross, P. N., Jr.; Jiang, X. D.; Villegas, I.; Weaver, M. J. *Electrochim. Acta* **1995**, *40*, 91.
(8) Sun, S. G.; Lipkowski, J.; Altounian, Z. *J. Electrochem. Soc.* **1990**, *137*, 2443.
(9) Xia, X. H.; Iwasita, T. J. *Electrochem. Soc.* **1993**, *140*, 2559.
(10) Climent, V.; Herrero, E.; Feliu, J. M. *Electrochim. Acta* **1998**, *44*, 1403.
(11) Lu, G. Q.; Crown, A.; Wieckowski, A. *J. Phys. Chem. B* **1999**, *103*, 9700.
(12) Smith, S. P. E.; Ben-Dor, K. F.; Abruña, H. D. *Langmuir* **2000**, *16*, 787.
(13) Sun, S. G.; Chen, S. P.; Li, N. H.; Lu, G. Q.; Chen, B. Z.; Xu, F. C. *Colloids Surf. A* **1998**, *134*, 207.
(14) Lin, W. F.; Christensen, P. A.; Hamnett, A. *Phys. Chem. Chem. Phys.* **2001**, *3*, 3312.
(15) Iwasita, T.; Dalbeck, R.; Pastor, E.; Xia, X. *Electrochim. Acta* **1994**, *39*, 1817.
(16) Pastor, E.; Castro, C. M.; Rodriguez, J. L.; Gonzalez, S. *J. Electroanal. Chem.* **1996**, *404*, 77.
(17) Chen, S. L.; Wu, B. L.; Cha, C. S. *J. Electroanal. Chem.* **1997**, *431*, 243.
(18) Bowker, M.; Bennett, R. A.; Poulston, S.; Stone, P. *Catal. Lett.* **1998**, *56*, 77.
(19) Capon, A.; Parsons, R. *J. Electroanal. Chem.* **1973**, *44*, 1.
(20) Mrozek, M. F.; Luo, H.; Weaver, M. J. *Langmuir* **2000**, *16*, 8463.
(21) Sun, S. G.; Lin, Y.; Li, N. H.; Mu, J. M. *J. Electroanal. Chem.* **1994**, *370*, 273.
(22) Sun, S. G.; Yang, Y. Y. *J. Electroanal. Chem.* **1999**, *467*, 121.
(23) Yang, Y. Y.; Zhou, Z. Y.; Sun, S. G. *J. Electroanal. Chem.* **2000**, *500*, 233.
(24) Yang, Y. Y.; Sun, S. G.; Gu, Y. J.; Zhou, Z. Y.; Zhen, C. H. *Electrochim. Acta* **2001**, *46*, 4339.
(25) Clavilier, J.; Fernandez-Vega, A.; Feliu, J. M.; Aldaz, A. *J. Electroanal. Chem.* **1989**, *258*, 101.
(26) Herrero, E.; Feliu, J. M.; Aldaz, A. *J. Electroanal. Chem.* **1994**, *368*, 101.
(27) Climent, V.; Herrero, E.; Feliu, J. M. *Electrochim. Acta* **1998**, *44*, 1403.
(28) Sun, S. G.; Chen, A. C.; Huang, T. S.; Li, J. B.; Tian, Z. W. *J. Electroanal. Chem.* **1992**, *340*, 213.
(29) Somorjai, G. A. *Chemistry in Two Dimensions*; Cornell University Press: Ithaca, 1981; p 163.
(30) Clavilier, J.; Faure, R.; Guinet, G.; Durand, R. *J. Electroanal. Chem.* **1980**, *107*, 205.
(31) Parson, R.; VanderNoot, T. *J. Electroanal. Chem.* **1988**, *257*, 9.
(32) Sun, S. G. In *Electrocatalysis*; Lipkowski, J., Ross, P. N., Eds.; Wiley-VCH: New York, 1998; p 243.
(33) Lamy, C.; Leger, J. M.; Clavilier, C.; Parsons, R. *J. Electroanal. Chem.* **1983**, *150*, 71.
(34) Yang, Y. Y. Ph.D. Dissertation, Xiamen University, 2000.
(35) Clavilier, J. J. *Electroanal. Chem.* **1987**, *236*, 87.
(36) Bard, A. J.; Faulkner, L. R. *Electrochemical Methods. Fundamentals and Applications*; John Wiley & Sons, Inc.: New York, 1980; p 167.
(37) Cha, Q. X. *Kinetics of Electrode Process*, 2nd ed.; Science Press: Beijing, 1987; p 143.
(38) Oldham, K. B. *J. Electroanal. Chem.* **1986**, *208*, 1.